PAP-512

Proc. Instn Civ. Engrs, Part 2, 1987, **83**, Mar., 295–314

PAPER 9136

WATER ENGINEERING GROUP

Behaviour of turbulent water jets in the atmosphere and in plunge pools

D. A. ERVINE, BSc, PhD, MICE, MIWES*

H. T. FALVEY, BS, MS, DrIng, MASCE†

The Paper describes measurements made on a free water jet discharging almost horizontally; from these, the Authors conjecture the fundamental nature of free turbulent jets plunging through the atmosphere and diffusing in the plunge pool. Consideration of jet diffusion in the plunge pool includes a comparison between submerged jet and impinging jet diffusion, the role of inner core decay for impinging jets in a pool, the effect of entrained air on the reduction of impact pressures, and an analysis of the pressure fluctuations caused by turbulence in the plunge pool shear layers.

Introduction

Turbulent water jets are frequently used in hydraulic structures to enhance energy dissipation and to promote air entrainment. A typical example of the use of jets to enchance energy dissipation is the spillway and plunge pool structure at Morrow Point Dam, Colorado (Fig. 1(a)). The spillway jets pass under sluice gates high up in the dam structure and plunge through the atmosphere, with almost vertical entry into the plunge pool. The jets diffuse in the concrete-lined plunge pool and the flow returns to the river course over the plunge pool end weir. It can be seen from the figure that the entire process is accompanied by a great deal of spray and aeration.

2. An example of turbulent water jets being used to promote aeration can be seen on spillway chutes (Fig. 2). In this case, the free jet produced at an aerator entrains sufficient air to eliminate cavitation damage. With this type of jet, aeration occurs on both the upper and lower surfaces of the nappe (Fig. 2).

3. Evidence of free surface aeration into the under-side of jets and nappes brings into question current thinking on the physical mechanism of aeration. Many investigators[1–4] have advocated the falling droplet hypothesis of aeration. With this hypothesis, turbulent energy close to the free upper surface of a flow overcomes surface tension and propels a droplet of water into the atmosphere. The droplet will in turn entrain an air bubble in its wake on impact with the free surface. This mechanism is clearly not possible on the under-side of a jet or nappe as a water droplet propelled out of the flow is unable to return to the flow, and yet a similar order of magnitude of air entrainment occurs at the upper and lower sides of the nappe. To account for aeration at the under-side of the nappe, other investigators[4,5] have proposed that spray is the principal entrainment mechanism.

Written discussion closes 15 May 1987; for further details see p. ii.

* Department of Civil Engineering, University of Glasgow.

† US Bureau of Reclamation, Division of Hydraulic Research, Denver, Colorado.

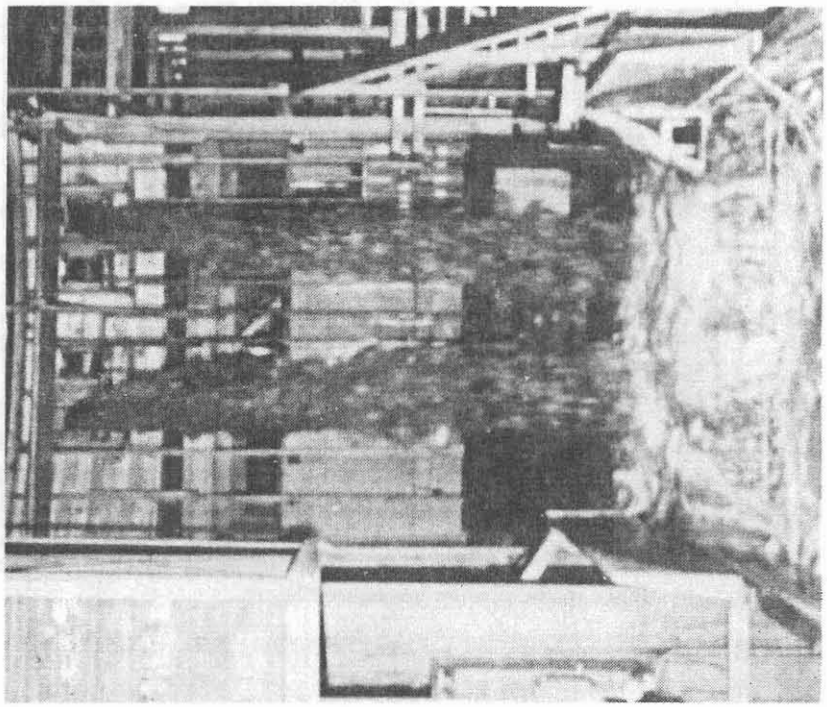

(b)

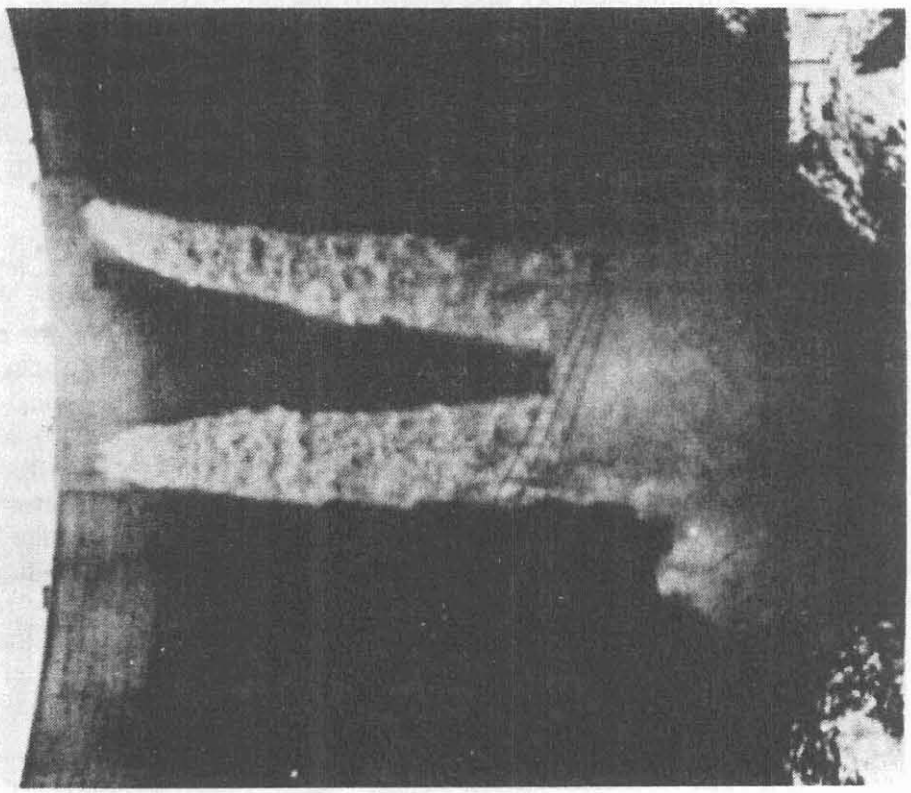

(a)

Fig. 1. Morrow Point Dam: (a) full-scale jets; (b) model jets (1 : 24 scale)

Notation

c	air concentration ($\beta/(1+\beta)$)
d	jet thickness (diameter) in atmosphere or plunge pool
d_i	jet diameter at impact
d_0	orifice diameter
g	gravitational constant
L	jet breakup length in the atmosphere
l'	turbulent eddy length
p	probability of encountering water outside jet solid core
$\bar{p}$	mean dynamic pressure of diffusing jet in the plunge pool
p'	root mean square fluctuating component of dynamic pressure in the plunge pool
Q	water discharge rate
Q_a	air flow rate in the plunge pool
Q_i	impact jet water discharge
R	radius of curvature of jet surface disturbances
Re	Reynolds number of flow (Ud/ν)
Tu	relative turbulence intensity (u'/U)
U	jet velocity in atmosphere or plunge pool
U_i	impact velocity of jet
U_o	average velocity of plane of orifice
$\bar{U}$	mean velocity at any cross-section in pool
u_b	air bubble rise velocity (0·25 m/s)
u'	root mean square value of axial component of turbulent velocity
v'	root mean square value of lateral component of turbulent velocity
We	Weber number of flow
X	distance from orifice
y	depth into plunge pool from free surface
y_c	depth of inner core decay
y_p	penetration depth of air bubbles in plunge pool
α	angles of jet diffusion in plunge pool
β	ratio of air flow to water flow
δ	lateral spread of jet
ε	amplitude of jet surface disturbances
ρ	density of water
σ	surface tension parameter
ν	kinematic viscosity

Subscripts

1	conditions in the inner region of jet core decay
2	conditions in the outer region of jet diffusion

However, this explanation does not account for the air observed moving into the body of the jet at the lower nappe. To account for the presence of air within the nappe, it has been proposed[6,7] that the air entrainment around free falling jets is due solely to the turbulent boundary layer of the water jet.

4. Although a clear understanding of the air entrainment process has not yet been developed, the direction is more towards a recognition of turbulence as the most significant air-entraining mechanism.[8] In any study of this nature, it is important that the physical nature of the phenomenon is considered. It is also important to investigate any major differences between model and prototype behaviour. For example, the free turbulent jets shown in (a) and (b) of Fig. 1 represent the behaviour of a prototype structure with Reynolds number approximately 3×10^7, and a 1 : 24 scale model with the jet Reynolds number of the

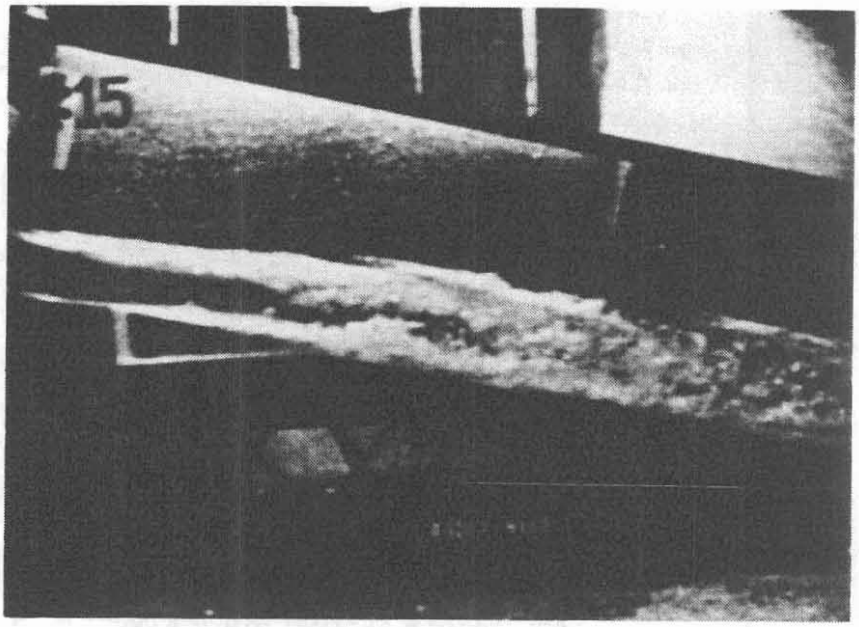

Fig. 2. Flow over air slot ramp; aeration on both sides of jet (Pinto[8])

order of 3×10^5. The lateral spreading of the plunging jet is approximately the same in both the model and the prototype. However, there is a major difference in the free surface aeration and spray at the plunge point between the model and the prototype. In addition, the prototype exhibits free surface aeration around the entire jet periphery.

5. It is argued that a detailed physical understanding of the processes involved will lead to a clearer understanding of the air-entraining mechanisms of free turbulent jets, the mean and fluctuating pressures at the plunge pool floor, and a more efficient plunge pool basin design.

Behaviour of water jets plunging through the atmosphere

6. Observations were made of a jet issuing horizontally from an orifice at the downstream end of a straight pipe. The test facility consisted of a high head pump, feeding both a bypass line to a flow control valve, a tee and a short section of straight pipe, and at the exit end a sharp-edged orifice of either 50 mm or 100 mm diameter (Fig. 3).

7. Longitudinal turbulence intensities and flow velocities were measured with a laser Doppler velocimeter. The water surface location was determined with a probability water surface probe.[9] Stroboscopic photography was used to obtain images of the jet surface.

8. The flow was adjusted to produce exiting jet velocities of 3·3 m/s, 5·0 m/s, 11·8 m/s, 17·7 m/s, 23·7 m/s and 29·6 m/s with the 100 mm orifice, and 5·0 m/s, 19·0 m/s and 28·5 m/s with the 50 mm orifice, giving a Reynolds number range of 2×10^5 to 2×10^6. Turbulence intensities in the jet varied between 1% and 9% depending on the straightening vanes placed in the upstream end of the straight pipe.

9. The physical properties of jets were found to vary greatly with the Reynolds number. This effect can be demonstrated by comparing the nature of the free surface of turbulent jets at velocities of 5 m/s and 25 m/s (Fig. 4).

10. With the 5 m/s jet, and a relative turbulence intensity of about 5%, the jet surface undulations are well rounded, indicating large diameter eddies close to the free surface. The turbulence intensity, Tu, is defined as

$$\mathrm{Tu} = u'/U$$

where u' is the root mean square value of the instantaneous axial velocity and U is the average axial velocity. Free surface aeration has not yet occurred. This jet is typical of a Froude scale model of a prototype plunging jet, where care has been exercised to simulate approximate prototype turbulence intensity.

11. The 25 m/s jet has a relative turbulence intensity of around 7%. The surface undulations of the jet exhibit a fine-grained turbulent structure superimposed on larger underlying eddies. The outward turbulent kinetic energy is about 50 times greater than for the 5 m/s jet, whereas the restraining surface tension has increased by a much lesser degree. The turbulent kinetic energy is defined as $\frac{1}{2}\rho u'^2$ and the restraining surface tension is $2\sigma/R$, where ρ is the density of water, σ is the interfacial surface tension and R is the radius of curvature of the jet undulations. In this case, the turbulent energy is high in small eddy lengths close to the free

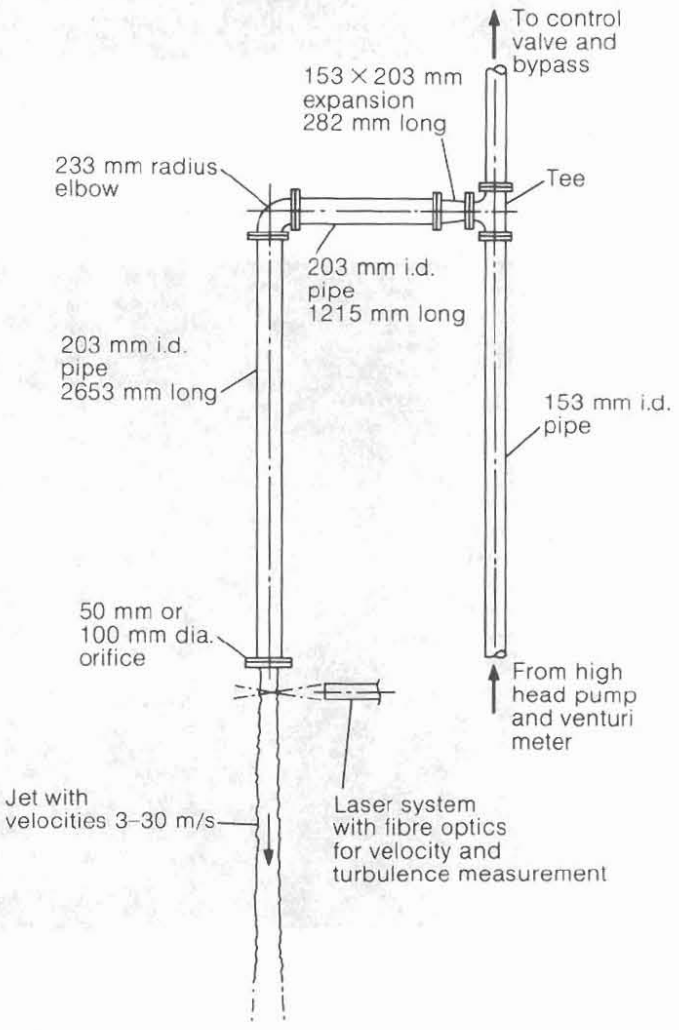

Fig. 3. Plan view of model

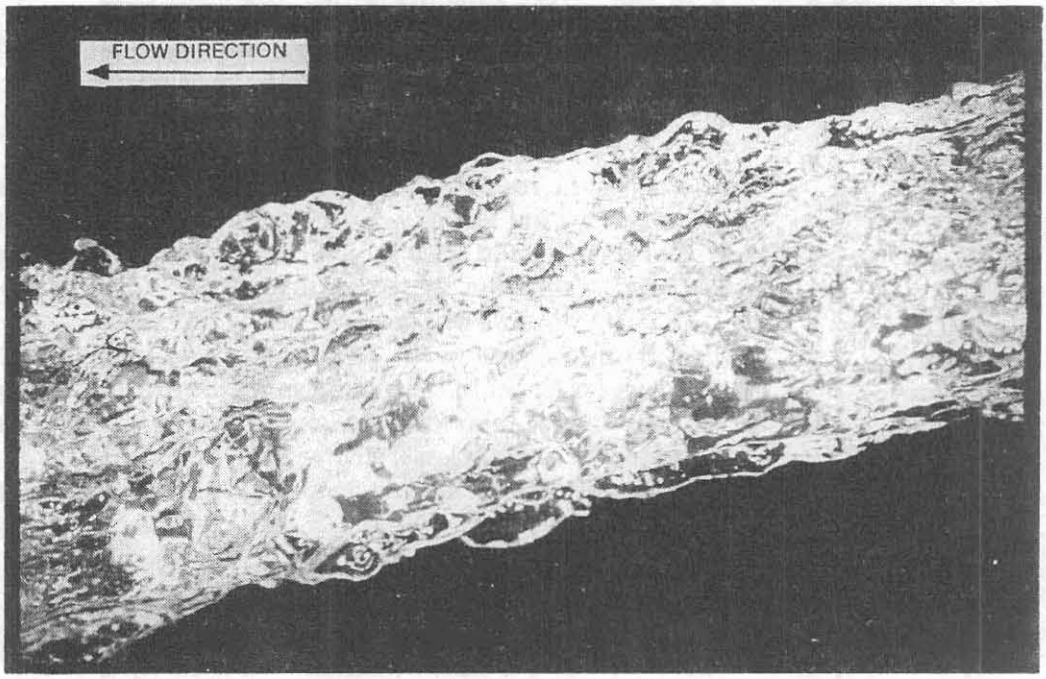

(a)

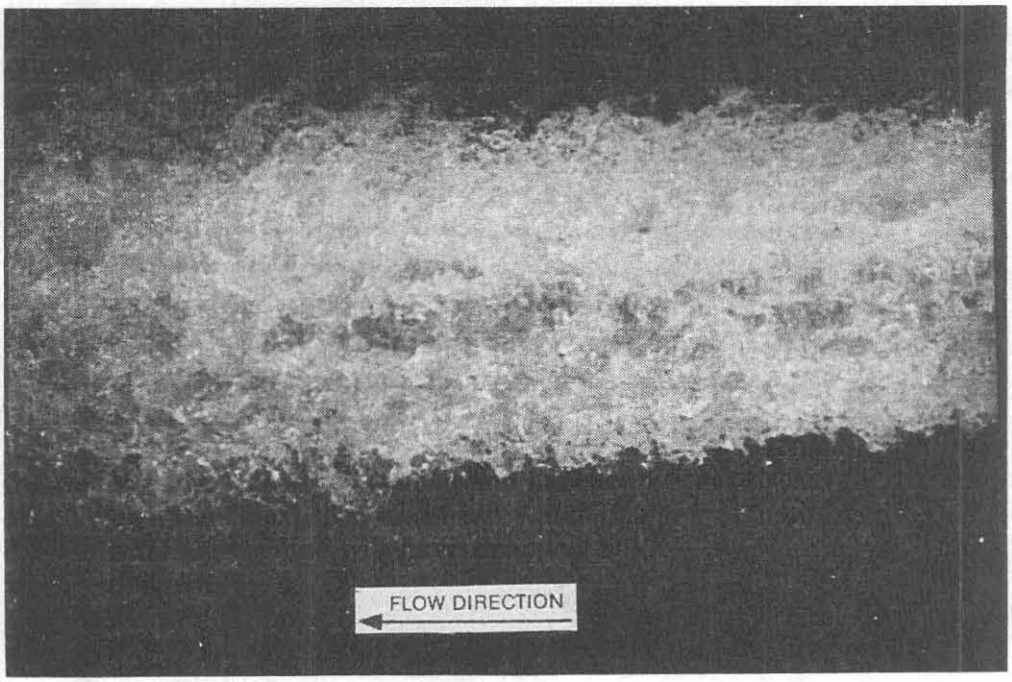

(b)

Fig. 4. Turbulent jets; flow from right to left; $d_o = 100$ mm: (a) $U = 5$ m/s, $Re \sim 4 \times 10^5$; (b) $U = 25$ m/s, $Re \sim 2 \times 10^6$

surface of the jet. Free surface aeration into the jet occurs as much on the lower side of the jet as the upper side, indicating that aeration does not occur by the falling droplet method, but by high intensity turbulent eddies close to the jet free surface.

12. The comparison of the two jet velocities highlights the great difficulty in modelling turbulent jets in the atmosphere. Even with comparable relative turbulence intensities, the high turbulent energy in the 25 m/s jet is able to cause aeration and spray, whereas there is little turbulent energy in smaller eddy lengths of the 5 m/s flow. The problem is that some important processes in free jets are dependent on Weber and Reynolds numbers and cannot be easily simulated in Froude models.

13. Important aspects of plunging jet behaviour are: the ability to spread laterally; the ability to become increasingly distorted during the plunge; and the ability to break up if the plunge length is sufficiently long. These aspects have a significant impact on the pressures experienced in the plunge pool basin, as disintegrated aerated jets produce much smaller mean pressures than intact, non-aerated jets.

14. To investigate the effect of turbulence on the spread, distortion and breakup of free jets, the axial turbulence intensity at the point of jet exit was related to the half angle of jet spread taken from high speed photographs. With limited data (Fig. 5), it appears that the rate of jet spread is given by

$$\delta_2/X = 0.38u'/U_o \tag{1}$$

where δ_2 is the lateral spread of the jet; X is the distance from the orifice; and U_o is the average velocity at the plane of the orifice.

15. If the outer edge is spreading in the manner indicated, then the inner core must be reducing in size in a predictable fashion. It has already been shown that the outer spread angle is proportional to the axial turbulence intensity. It could be argued that δ_2/X is equal to the lateral component of turbulence intensity v'/U_o.

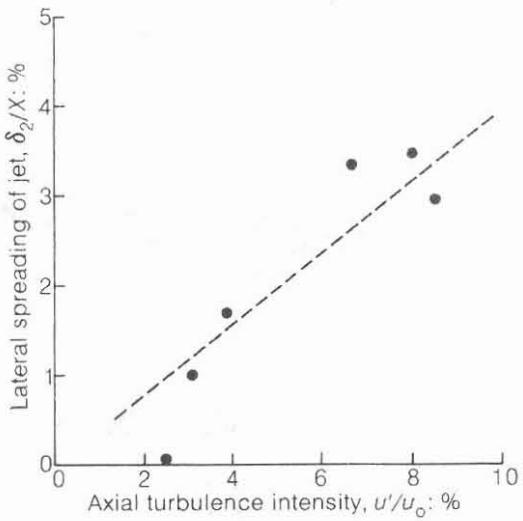

Fig. 5. Dependence of lateral jet spreading on turbulence intensity acting at orifice outlet

Assuming negligible velocity change over a short distance of the high velocity jet, continuity between sections 1 and 2 of Fig. 6 gives

$$U_o d_o^2 \sim U_o d^2 + (P_1/100)U_o(d_o^2 - d^2) + (P_2/100)U_o(d_e^2 - d_o^2) \tag{2}$$

where P_1 is the percentage probability of encountering water in the δ_1 region and P_2 is the percentage probability of encountering water in the δ_2 region.

16. Ignoring second order terms, the ratio of the magnitude of inner core decay to the outer core spread is given by

$$\delta_1/\delta_2 = P_2/(100 - P_1) \tag{3}$$

Equation (3) is valid only for the case of a high velocity jet not contracting under the influence of gravity.

17. An estimate made for δ_1/δ_2 was obtained from probability measurements made at the edge of typical jets. A probability probe showed that the edge of a jet follows approximately a Gaussian distribution (Fig. 7). This is not surprising as the jet surface disturbances are caused by turbulent fluctuations within the jet, which in turn also follow a Gaussian distribution. Initial estimates of δ_1/δ_2 from probability data reveal that for high velocity jets with negligible contraction due to gravity, the value of δ_1/δ_2 is approximately $\frac{1}{5}$ to $\frac{1}{7}$.

18. Thus the angle of jet core decay may be as small as 15–20% of the angle of lateral spread, ignoring core contraction due to gravity. Photograph (b) of Fig. 4 may be misleading in the sense that the jet appears intensely rough and aerated. However, it is likely that it contains a substantial inner core not immediately visible. For a typical outer spread δ_2/X of 3–4%, corresponding to a turbulence intensity u'/U of 5–8%, the inner core decay (δ_1/X) can be as small as $\frac{1}{2}$–1%.

19. If a jet begins to break up or to disintegrate when the inner core decays completely, the jet breakup length (L) is given approximately by

$$\delta_1/X \sim \tfrac{1}{2}\text{–}1\% = (d_o/2)/L \tag{4}$$

or

$$L/d_o \sim 50\text{–}100 \tag{5}$$

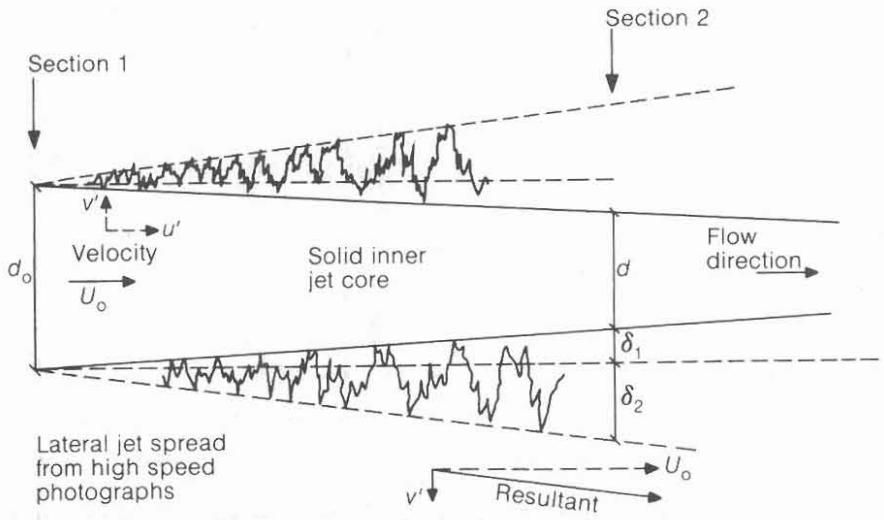

Fig. 6. Spreading turbulent jet; total jet diameter at section 2 is $d_e = d + 2\delta_1 + 2\delta_2$

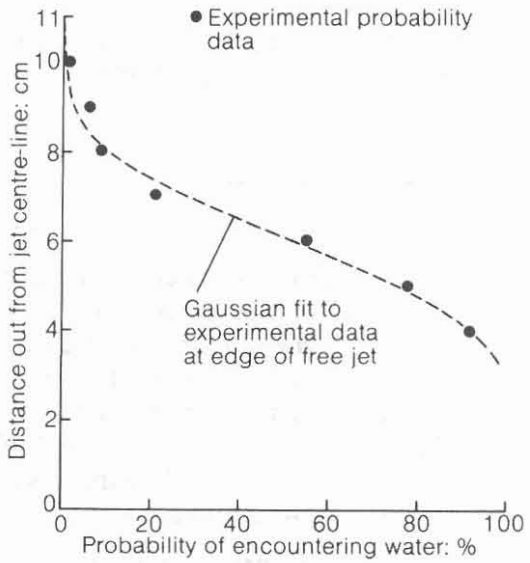

Fig. 7. Probability of encountering water outside the solid core of a plunging turbulent jet

for rough turbulent jets. This empirical estimate of the breakup length of circular jets agrees with previous experimental data.[10] For a plunging jet of 25 mm diameter with a relative turbulence intensity between 3% and 8%, the ratio of the breakup length to the jet diameter at the nozzle varies between 50 and 100 (Fig. 8). It is apparent that the initial turbulence intensity (Tu) is the most important factor in determining the jet breakup length. This is because the initial turbulence intensity determines the degree of lateral jet spread and by continuity controls the rate of inner core decay of the jet, which in turn determines the eventual breakup of the jet.

20. Since the jet spreads laterally at a rate proportional to the turbulence intensity u/U, the jet particles moving perpendicular to the flow must have adequate kinetic energy to overcome the restraining surface tension. Representing the

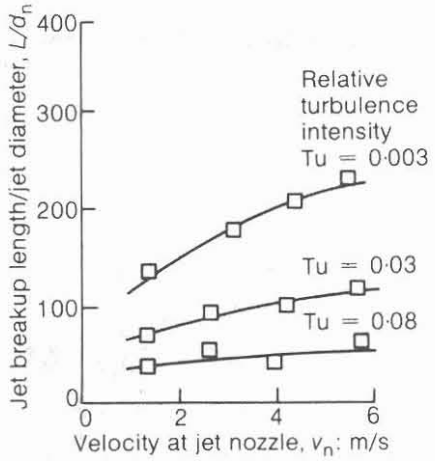

Fig. 8. Variation in plunging jet breakup length with turbulence intensity; nozzle diameter = 25 mm

lateral turbulent kinetic energy as $\frac{1}{2}\rho v'^2$ and the restraining surface tension pressure as $2\sigma/R$ (Fig. 9), the criterion for jet spreading is

$$\tfrac{1}{2}\rho v'^2 \geqslant 2\sigma/R \tag{6}$$

or from equation (1)

$$\tfrac{1}{2}\rho u'^2 \geqslant 13{\cdot}8\sigma/R$$

where R is the radius of curvature of a jet surface undulation.

Equation (6) must also be one criterion for the onset of free surface aeration, as air bubbles will not be entrained across the free surface until there is sufficient turbulent energy relative to the surface tension forces.

21. A further criterion for the onset of aeration concerns the value of R, the radius of curvature of surface undulations. An estimate of the value of R can be obtained making the following assumptions, based partly on observations from high speed photographs.

(*a*) At the onset of aeration, the radius of the eddies in the jet have the same order of magnitude as the surface distrubance amplitude (Fig. 9).

(*b*) The magnitude of the surface disturbances are proportional to the kinetic energy of the turbulent fluctuations $u'^2/2g$, as advocated by Sene.[2]

22. Thus from equation (6), assuming isotropic turbulence meantime,

$$R \geqslant 4\sigma/\rho u'^2 \sim \varepsilon \sim u'^2/2g \tag{7}$$

giving

$$u'^4 \sim 8\sigma g/\rho \tag{8}$$

or

$$u' \sim 0{\cdot}275 \text{ m/s at } 10°\text{C}$$

as an estimate of conditions for the onset of free surface aeration. Equation (8) may be also expressed in the form of the jet velocity

$$U = \frac{0{\cdot}275}{u'/U} = \frac{0{\cdot}275}{\text{Tu}} \tag{9}$$

where U is the jet velocity at the onset of aeration.

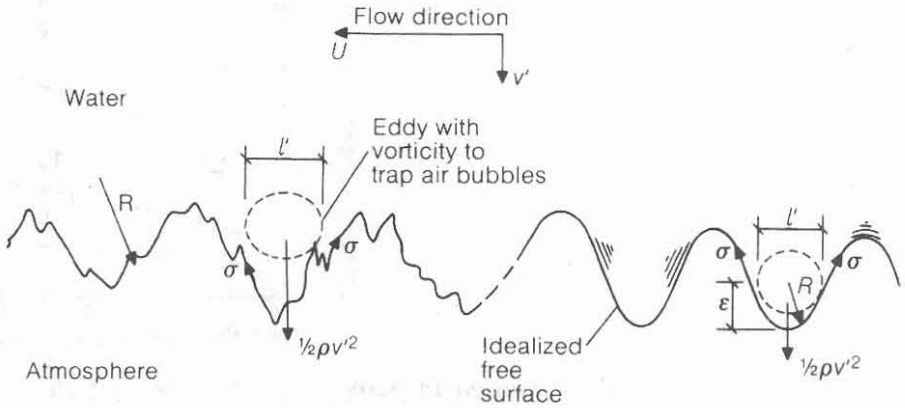

Fig. 9. Free surface with definition of physical parameters

23. Equation (9) might be applied to other situations involving free surface aeration. Spillway chute flow, for instance, generally produces aeration when the boundary layer approaches the free surface. At that point, the turbulence intensity (Tu) is generally of the order 4–5%, and hence equation (9) would produce a required flow velocity of $U = 5{\cdot}5$–7 m/s for the onset of aeration.

24. With reference to the Morrow Point Dam spillway example (Fig. 1), the reason for the difference between the appearance in the model and the prototype jets can be seen immediately. With a relative turbulence intensity of approximately 4–5% in each case, a jet velocity of 5·5–7 m/s would be required for aeration. The model jet exits at velocities much less than 5 m/s, whereas the prototype has an exit velocity around 10 m/s.

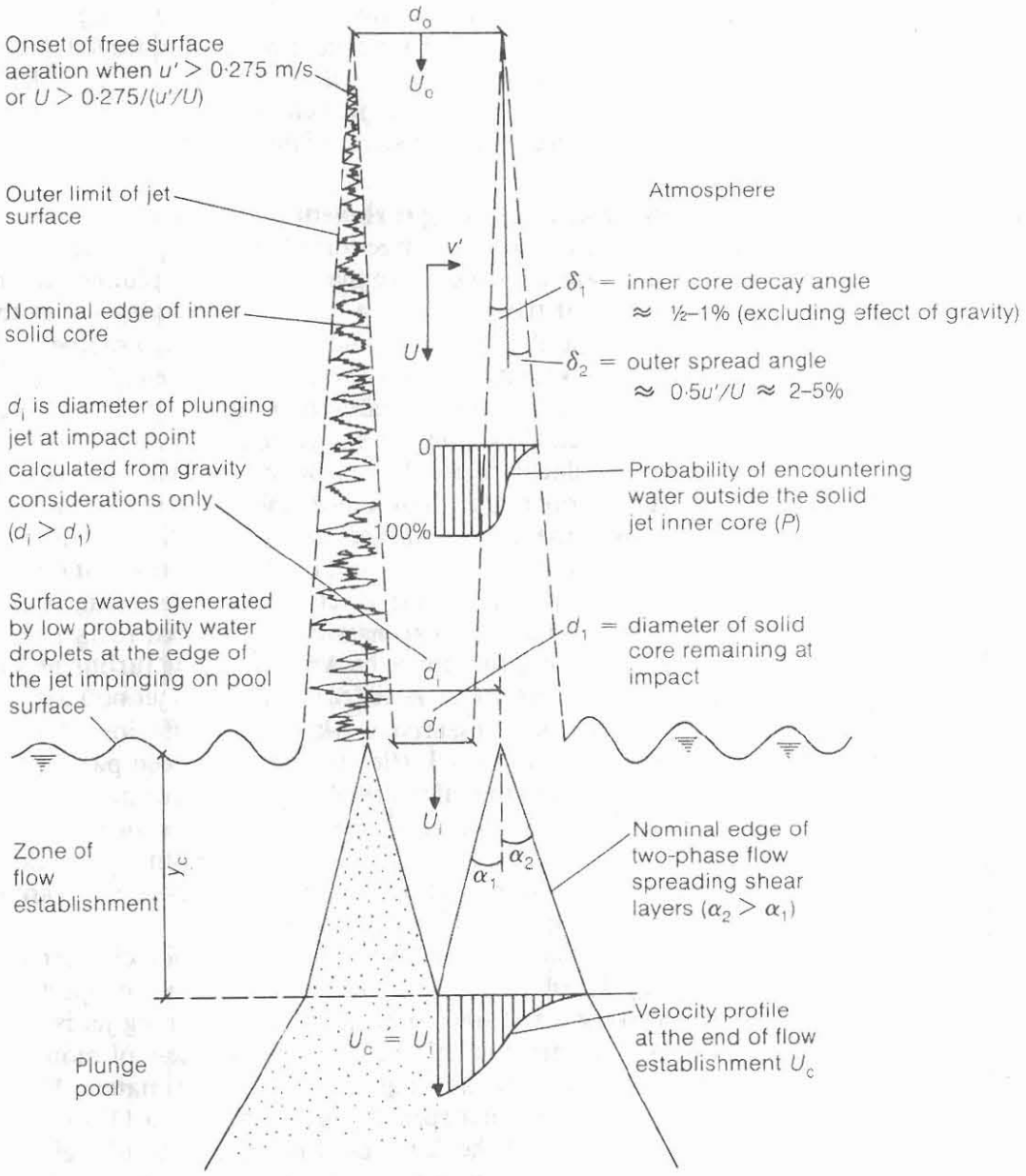

Fig. 10. Jet in atmosphere and in plunge pool

25. The characteristics of free turbulent jets can be summarized as follows.

26. The initial turbulence intensity determines the angle of lateral spread of the jet. Thus if a water particle at the edge of the jet experiences an axial velocity U, and a root mean square lateral velocity fluctuation v', then the resultant angle of motion is proportional to $\tan(v'/U)$. Initial estimates give

$$v'/U_o \sim 0{\cdot}4\text{–}0{\cdot}5u'/U_o \tag{10}$$

27. If the outer angle of spread is known, then by continuity, the inner core decay angle can be determined. This can be as small as 15–20% of δ_2, giving typical values of δ_1 in the region of $\frac{1}{2}$–1%.

28. The probability of encountering water outside the inner solid jet core is given approximately by Gaussian distribution.

29. The eventual breakup or disintegration length of a jet is given by $L/d_o \sim$ 50–100. At this point, the inner core will have decayed to zero.

30. Free surface aeration will occur when the turbulent velocity at the edge of the jet $u' \sim 0{\cdot}275$ m/s, or the jet velocity $U \sim 0.275/\mathrm{Tu}$, where Tu is the turbulence intensity. These characteristics are illustrated in the upper part of Fig. 10.

Diffusion of a plunging turbulent jet in a pool

31. The nature of the free turbulent jet requires careful consideration when the flow mechanisms which take place within the plunge pool are being analysed. It is apparent that the surface of a turbulent plunging jet, at the point of impact with the plunge pool, is irregular and will not have a diameter d_i, calculated purely on the basis of gravity acting over the plunge length. Instead, the jet may have an inner core region and an undulating outer region. The outer region may or may not be aerated, depending on the velocity and the turbulence intensity. On account of the irregularity of the flow in the outer region, it will produce surface waves in the plunge pool rather than well-defined penetrating shear layers (Fig. 10).

32. Because of the surface waves and the irregular outer region of the jet, conventional shear layers cannot exist in the steady state (α_1 and α_2 of Fig. 10). The point of origin of the shear layers will at one instant be as close together as the solid core, and at the next instant be displaced towards the outer edge of the jet. This is one major difference between plunging turbulent jet shear layers and those of submerged jets: in the latter case, the initial jet boundary is clearly defined.

33. Most past research work on the diffusion of jets has been confined to submerged entry cases. Little attention has been paid to the more complex problems arising from the influence of impinging free turbulent jets and air entrainment on the diffusion process. Recent work[11] has provided useful insights into the behaviour of jet diffusion in plunge pools, both for the case of no air entrainment and with air entrainment (Fig. 11(b)–(d)). These studies are summarized below and their areas of applicability are outlined.

34. The case of submerged jet diffusion for circular jets[12] will be considered first (Fig. 11(a)). In this case, the jet entering has properties identical with those of the receiving water and the edge of the incoming jet is clearly defined. A zone of flow establishment is defined where the process of momentum transfer causes an inner core decay at an angle (α_1) of approximately $4\frac{1}{2}°$, and an outer nominal spread of 6°. The outer spread angle increases to 11° (or 1 in 5 slope) in the zone of established flow. If the data could be applied to plunging free jets, then the inner core would remain up to $y/d_i \sim 6{\cdot}2$, where y is the depth into the plunge pool and d_i the jet diameter at impact.

35. The second case deals with an almost laminar plunging jet (turbulence intensity $u'/U \sim 0{\cdot}3\%$) but with the entry velocity low enough to give zero air entrainment (Fig. 11(b)). The angles of core decay and outer spread in the zone of flow establishment are very similar to those of a submerged jet, although marginally greater. This type of plunging jet is not typical of either prototype behaviour or most model study behaviour.

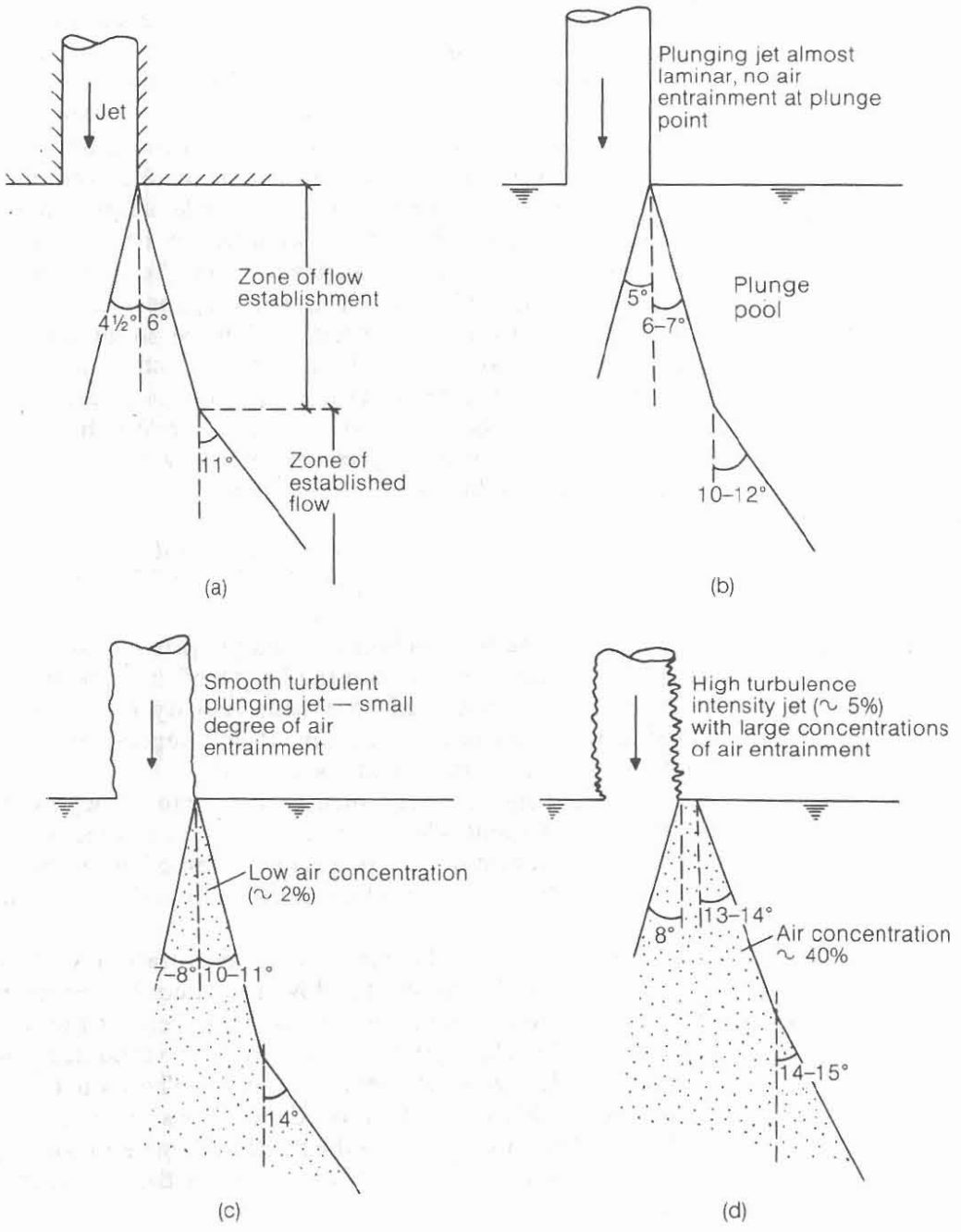

Fig. 11. Jet diffusion in the plunge pool for single-phase and two-phase shear layers: (a) submerged jet (Albertson et al.[12]); (b) almost laminar plunging jet (McKeogh[11]); (c) smooth turbulent plunging jet (McKeogh[11]); (d) highly turbulent plunging jet

36. The third case illustrates the behaviour of jet diffusion for a smooth turbulent impinging jet (turbulence intensity $u'/U \sim 1{\cdot}2\%$) when a low concentration of air is entrained ($C \leqslant 2\%$) (Fig. 11(c)). It is very interesting to note a 50% increase in both the angle of inner core decay and outer jet spread in the zone of flow establishment. This has important implications for predicting pressures on plunge pool floors, as the inner core would have decayed completely by $y/d_i \sim 4$. The large increase in α_1 and α_2 is not attributable to the volume of air contained in the shear layer but to the large increase in turbulence level in the shear layer stemming from the uneven plunging jet surface.

37. The last case is the most relevant to both prototype and most model situations (Fig. 11(d)). The impinging jet is essentially rough turbulent ($u'/U \sim 5\%$), and large air concentrations of the order of 40% are entrained. Measurements of the outer angle of spread in the zone of flow establishment yield average values of around 13–14°. The angle of inner core decay α_1 has not yet been measured successfully but is estimated to be around 8°. This is based on an approximate momentum balance between the jet at the point of impact and at the end of the zone of flow establishment (Appendix 1).

38. It is reasonable to speculate that the presence of air bubbles in the diffusing plunge pool shear layers will result in a reduction in mean dynamic pressures. This can be shown by approximating the two-phase spreading shear layer flow with a pseudo-fluid whose density is $(1 - \bar{c})\rho$, where $\bar{c}$ is the mean air concentration. Thus the ratio of the dynamic pressure including air bubbles to the dynamic pressure excluding air bubbles would be given by

$$\frac{\bar{p}}{\frac{1}{2}\rho U^2} = \frac{\frac{1}{2}\rho(1 - \bar{c})U^2}{\frac{1}{2}\rho U^2} = (1-\bar{c}) \tag{11}$$

39. Maximum reduction of dynamic pressure by entrained air is achieved at pool depths just greater than the length of the zone of flow establishment. Up to that point, an unaerated core with velocity U_i still exists. Thus the ability to predict the effect of air entrainment will depend on accurate calculations of the mean air concentration at any pool depth.

40. The conditions at which air entrainment begins in the plunge pool can be estimated. At point where the jet enters the plunge pool, turbulent intensities of 25–30% are common. For these intensities, equation (9) predicts a minimum flow velocity for the inception of air entrainment of 1 m/s, which is in agreement with observations.[10]

41. Estimates of the mean air concentration with depth can be made by assuming that the mean air flow rate decays approximately linearly from a maximum value at the jet plunge point to zero at the maximum air bubble penetration depth. This variation follows the observed decay in water velocities in the established flow zone of submerged jets.[12] The reduction in the mean concentration is due to detrainment out of edges of the spreading jet.

42. A theoretical value of the maximum penetration depth of air bubbles in an unconfined pool can be obtained by using the continuity equation for diffusing circular jets[12]

$$Q/Q_i \sim 0.32Y/d_i \tag{12}$$

where Q is the water discharge at any cross-section within the zone of established flow ($Q = (\pi/4)d^2\bar{U}$); Q_i is the impact jet water discharge ($Q_i = (\pi/4)d_i^2 U_i$); $\bar{U}$ is the

mean velocity at any cross-section in the pool; and d is the total width of the shear layer at that point.

43. The shear layer width can be given by

$$d = d_i + 2y \tan \alpha_2 \tag{13}$$

at the point of maximum air bubble penetration $y = y_p$, and the mean water velocity can be approximated by the bubble rise velocity

$$\bar{U} \sim u_b \sim 0{\cdot}25 \text{ m/s} \tag{14}$$

44. Combining equations (12)–(14) gives an expression for the penetration depth (y_p) in the form

$$U_i/u_b = 3{\cdot}12[d_i/y_p + 4 \tan \alpha_2 + (4y_p/d_i) \tan^2 \alpha_2] \tag{15}$$

The equation agrees well with empirical data,[13] as shown in Fig. 12.

45. When the maximum penetration of air bubbles in an unconfined pool has been established, an approximate relationship for the mean air concentration at any point within the pool depth can be developed. From this, the mean dynamic pressure at any point can be determined.

46. It should be assumed that the water discharge rate in the shear layer increases as a result of entrainment from the surrounding body of water, as given by

$$Q \sim 0{\cdot}32(y/d_i)Q_i \tag{16}$$

If the initial air flow rate into the shear layer at the point of jet impact is given by Q_{ai}, then its relationship to the initial water discharge is given by

$$Q_{ai} = \beta_i Q_i \tag{17}$$

The value of β_i is the air/water ratio at jet impact, and has an upper limit of about 3. This corresponds to an upper limit air concentration of 0·75, since $c = \beta/(1 + \beta)$.

47. The assumption that the total air flow rate (Q_a) decreases linearly with depth into the pool can be expressed as

$$Q_a = Q_{ai}(1 - y/y_p) \tag{18}$$

where y is any pool depth less than the maximum air bubble penetration depth y_p.

48. Combining equations (16)–(18) results in an expression for the air/water ratio (β) at any pool depth

$$\beta = 3{\cdot}12\beta_i(d_i/y - d_i/y_p) \tag{19}$$

or

$$\beta = 3{\cdot}12\beta_i(1 - y/y_p)$$

49. From equation (19), the ratio of the dynamic pressure including air entrainment to the dynamic pressure excluding air entrainment is given by

$$\frac{\bar{p}}{\frac{1}{2}\rho U^2} = \frac{1}{1 + 3{\cdot}12\beta_i(d_i/y - d_i/y_p)} \tag{20}$$

where values of d_i/y_p are given in Fig. 12.

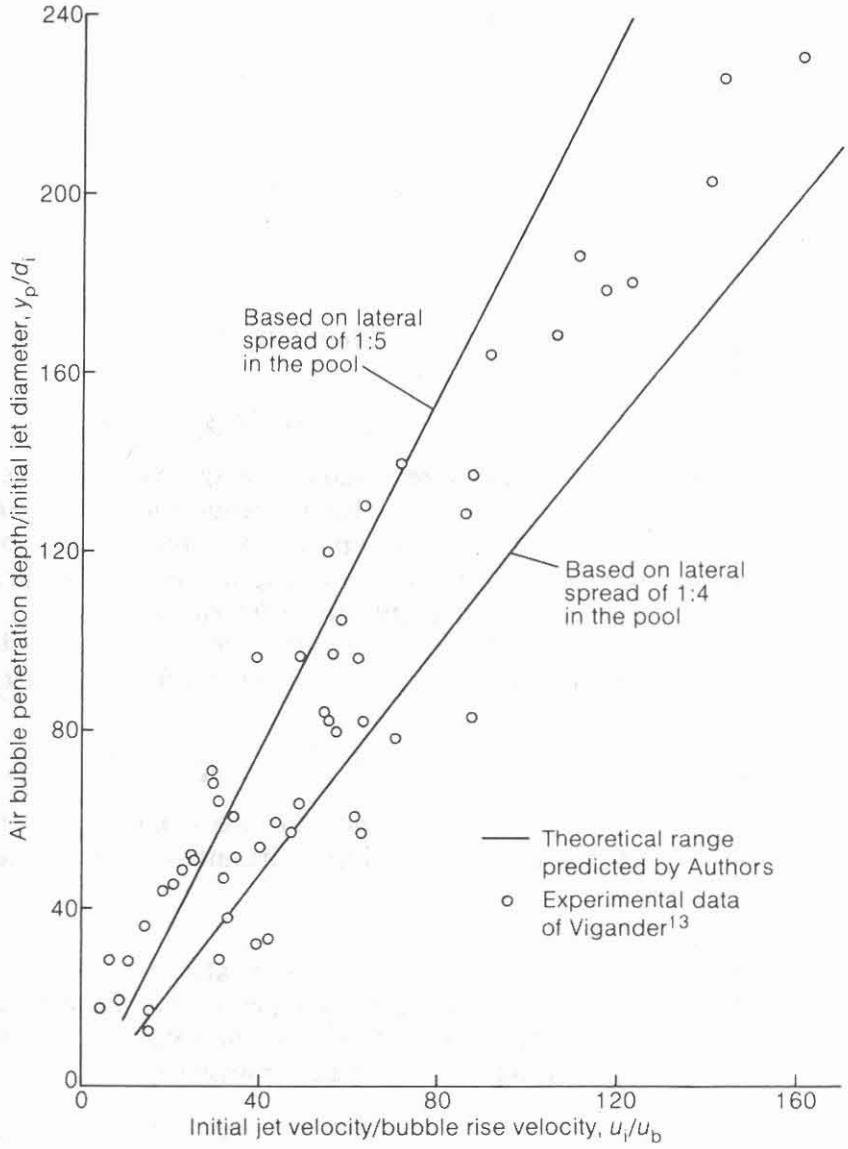

Fig. 12. Penetration depth of air bubbles in an unconfined pool (bubble rise velocity u_b to be taken as 0·25 m/s)

50. The pressure reduction due to air entrainment given by equation (20) has not been verified by experimental results. It is dependent on the assumption of linear decay in total air flow rate with depth and on estimates of the plunge point ratio of air flow to water flow, β_i. Hence equation (20) should be used only for estimation.

51. The value of the air/water ratio at jet impact can be estimated from the premise that β_i varies with $(L/d_0)^{1/2}$, where L is the plunge length through the atmosphere and d_o is the nozzle diameter. The upper limit of β_i is approximately 3. Thus

$$\beta_i = K(L/d_o)^{1/2} \tag{21}$$

for vertical plunging jets, with the value of K given from Table 1.

Table 1. Approximate values of K

	Circular jets	Wide rectangular jets	Valid range
Rough turbulent	0·4	0·2	$L/d_o \leqslant 50$
Moderate turbulent	0·3	0.15	$L/d_o \leqslant 100$
Smooth turbulent	0·2	0·1	$L/d_o \leqslant 200$

52. Returning to equation (11), the mean dynamic pressure acting at any point on the plunge pool floor is given by

$$\bar{p} = (1 - \bar{c})\tfrac{1}{2}\rho U^2 \tag{22}$$

where $\bar{c}$ is the air concentration and U the vertical velocity component at that point.

53. For plunge pool basins shallower than the zone of flow establishment, the value of U should be taken as the impact velocity U_i, and c may be taken as zero, because of the unaerated solid core. For this case, $\bar{p} = \frac{1}{2}\rho U_i^2$; that is, the mean pressure may be as high as the full reservoir head.

54. For plunge pools deeper than the zone of flow establishment, $y > y_c$, equation (22) applies, but requires judicious assessment of suitable values of $\bar{c}$ and U.

55. Equations (15), (20) and (21) can be used to estimate the air concentration. Suitable values for velocity U will depend on the assumption of linear velocity decay with depth in the zone of established flow, and will also depend on an accurate judgment of the depth of inner core decay, y_c. It has already been established that the inner decay angle is of the order 7–9°, giving a conservative value of y_c of $4d_i$. Using these assumptions the velocity U at any depth greater than y_c is given by

$$U \sim 4U_i d_i/y \tag{23}$$

and hence the mean dynamic pressure ($y > y_c$) would be given by

$$\bar{p} \sim (1 - \bar{c})\tfrac{1}{2}\rho U_i^2[16(d_i/y)^2] \tag{24}$$

56. Two important comments are required concerning this expression. The value of y_c is estimated as $4d_i$, where d_i is the calculated jet diameter at impact. In fact, no such diameter exists; the inner core can be decaying from a jet diameter as small as the plunging jet solid inner core, $d_1 < d_i$, and can also be decaying from a jet diameter almost as large as the outer jet edges. This will result in an oscillating value of y_c which may be much less than $4d_i$ and also much greater than $4d_i$. This phenomenon is currently under investigation.

57. Another important point concerns the fact that Froude scale models must overestimate mean dynamic pressures, compared with a prototype. In the atmosphere, jet spreading, inner core decay and free surface aeration are affected considerably by turbulence intensity, Reynolds number and Weber numbers, resulting in a more diffuse prototype jet at the point of impact with the plunge pool. Furthermore, a prototype jet will invariably have greater air concentrations in the shear layer in the plunge pool. Both sets of factors ensure mean prototype pressures are significantly less than model pressures.

Appendix 1. Estimation of diffusion core dimensions by the momentum equation

58. Consider the case of a vertical free circular turbulent jet with air entrainment around the jet periphery entering a plunge pool (Fig. 13), where ρ is the density of the solid water jet, $(1 - c)\rho$ is the density of the aerated shear layer, c is the air concentration, α_2 is the angle of the outer core spread and α_1 is the angle of inner core decay.

59. Momentum of entering jet is

$$\rho(\pi/4)d_i^2 U_i^2 \tag{25}$$

assuming a uniform jet velocity at entry. Momentum of the jet at the end of flow establishment ($y = y_c$) is approximated to

$$\rho(1 - \bar{c})(\pi/4)(d_i + 2y_c \tan \alpha_2)^2 \bar{U}_c^2 \tag{26}$$

where $\bar{c}$ is the mean concentration of air at this level and $\bar{U}_c$ is the mean velocity. Using the principle of similarity of velocity profiles $\bar{U}_c = KU_{c,\max} = KU_i$, and combining (25) and (26) gives

$$(1 - \bar{c})[1 + (2y_c/d_i) \tan \alpha_2]^2 K^2 = 1 \tag{27}$$

Now $\tan \alpha_1 = d_i/2y_c$, and substituting into equation (27) gives

$$(1 - \bar{c})(1 + \tan \alpha_2/\tan \alpha_1)^2 K^2 = 1 \tag{28}$$

60. The value of K can be estimated from the case when $c = 0$.[12] For this case, $\tan \alpha_2/\tan \alpha_1 = \tan 6°/\tan 4\frac{1}{2}° = 4/3$, giving $K = 0{\cdot}428$ at the end of the zone of flow establishment.

61. The value of $\bar{c}$ in equation (28) needs to be estimated. For circular jets, the flow at the end of the zone of flow establishment, $Q/Q_i \sim 2$. The additional entrainment of water gives a

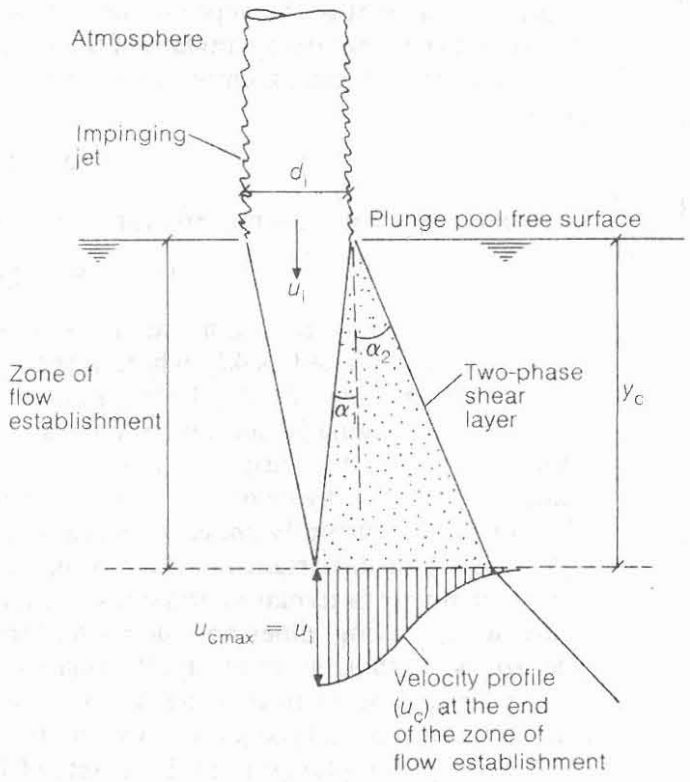

Fig. 13. Definition sketch of parameters

Table 2

Air concentration (c), %, at point of jet entry	α_2/α_1
0	1·333
2	1·37
20	1·5
40	1.72
50	1.88

water discharge twice that at the point of jet entry. This would imply that an air concentration of $c = 40\%$ for instance, at the point of jet entry, would give an air concentration of 25% at the end of the zone of flow establishment, as the ratio of air flow to water flow would be halved. This approach assumes continuity of air flow in the zone of flow establishment.

62. Equation (28) can now be used to determine the effect of air entrainment on the value of α_2/α_1. Results are shown in Table 2.

63. The validity of Table 2 can be tested in the light of experimental data shown in Fig. 11. For the case of no air entrainment (Fig. 11(b)), α_2/α_1 should remain 1·33; this is borne out by the data, as $6–7°/5° = 1·2–1·4$. For the case of 2% air concentration (Fig. 11(c)), α_2/α_1 should be 1·37: the observed values are $10·5°/7·5° \sim 1·4$.

64. For the case of rough turbulent jets with high air concentrations, measured values of α_2 are of the order of 14° (Fig. 11(d)). The inner core angle α_1 has not been measured to date, but by implication (Table 2) $\alpha_2/\alpha_1 \sim 1·5–1·9$ for high concentrations. Thus α_1 is in the range 7–9°.

65. Therefore, with impinging turbulent jets having substantial air entrainment, the angle of inner core decay is of the order of 7–9°. This is substantially higher than the value of $4\frac{1}{2}°$ from submerged jet data. Furthermore, the jet inner core will decay to zero at values of y_c/d_i of the order of 3–4 and not the value of 5.[14] This has important implications in determining pressures on plunge pool floors.

References

1. Rao N. S. L. and Kobus H. (Eds). *Characteristics of self-aerated free surface flow*. Erich Schmidt, Berlin, 1975, 67–88.
2. Sene K. J. *Aspects of bubbly two-phase flow*. PhD thesis, Trinity College, Cambridge, 1984.
3. Volkart P. The mechanism of air bubble entrainment in self aerated flows. *Int. J. Multiphase Flow*, 1980, **6**, 411–423.
4. Rabban S. L. and Rouve G. Beluftung von Grundablassen. *Wasserwirtschaft*, 1985, **75**, No. 9, 393–398.
5. Pinto N. L. de S. *et al.* Aeration at high velocity flows. *Int. Wat. Pow. Dam Constr.*, 1982, Feb., 34–38; Mar., 42–44.
6. DeFazio F. G. and Wei C. Y. Design of aeration devices on hydraulic structures. *Proc. Conf. on Frontiers of Hydraulic Engineering, 1983*. American Society of Civil Engineers, Hydraulics Specialty Conf., 426–431.
7. Glazov A. J. Calculation of the air-capturing ability of a flow behind an aerator ledge. *Hydrotech. Constr.*, 1985, **18**, May, No. 11, 554–558 (a translation from *Gidrotekhnicheskoe Stroitel 'stvo*, 1984, No. 11, Nov., 37–39.
8. Pinto N. L. de S. Model evaluation of aerators in shooting flow. *Symp. on Scale Effects in Modelling Hydraulic Structures, 1984*. International Association for Hydraulic Research, Esslingen, W. Germany.
9. Falvey H. T. *Air-water flow in hydraulic structures*. US Bureau of Reclamation, Denver, Colorado, 1980, Engineering Monograph 41.
10. Ervine D. A. *et al.* Effect of turbulence intensity on the rate of air entrainment by plunging water jets. *Proc. Instn Civ. Engrs*, Part 2, 1980, **69**, June, 425–445.

11. McKeogh E. J. *A study of air entrainment using plunging water jets.* PhD thesis, Queen's University, Belfast, 1978.
12. Albertson M. L. *et al.* Diffusion of submerged jets. *Proc. Am. Soc. Civ. Engrs*, 1948, **74**, 639–663.
13. Vigander S. Bubbles, drops and friction on the judgement scale. *Symp. Scale Effects in Modelling Hydraulic Structures, 1984.* International Association for Hydraulic Research, Esslingen, W. Germany. Paper 5.1.
14. Hausler E. Spillways and outlets with high energy concentration. *Trans. Int. Symp. on Layout of Dams in Narrow Gorges, 1983*, **2**, ICOLD, Rio de Janeiro.

Bibliography

King D. L. *Hydraulic model studies for Morrow Point Dam.* US Bureau of Reclamation, Denver, Colorado, 1967, Engineering Monograph 37.

Novak P. (Ed.). *Developments in hydraulic engineering.* Elsevier Applied Science, London, 1984, **2**, Chapter 5.

Rajaratnam N. (Chow V. T. (Ed.)). Hydraulic jumps. *Advances in hydroscience.* Academic Press, New York, 1967, **4**, 198–280.